Quantification of inflammatory cellular responses using real-time polymerase chain reaction

LeeAnn O. Bailey, Newell R. Washburn, Carl G. Simon, Jr., Edward S. Chan, Francis W. Wang
Biomaterials Group, Polymers Division, National Institute of Standards and Technology, Gaithersburg, Maryland 20899-8545

Received 11 April 2003; revised 18 November 2003; accepted 20 November 2003
Published online 9 March 2004 in Wiley InterScience (www.interscience.wiley.com). DOI: 10.1002/jbm.a.20134

Abstract: The introduction of tissue engineering strategies for the repair and replacement of human body components extends the application and importance of biomaterials. Implanted biomaterials frequently evoke inflammatory responses that are complex and not well understood at present. The goals of this work were to develop improved measurement methods for the quantification of cellular inflammatory responses to biomaterials and obtain data that lead to an enhanced understanding of the ways in which the body responds to the introduction of biomaterials. To evaluate the biocompatibility of materials, we established a system that allows for the analysis and quantitation of cellular inflammatory responses *in vitro.* In this study, the inflammatory responses of murine macrophages (RAW 264.7) were analyzed. The cells were incubated with polymethylmethacrylate (PMMA) microspheres in the presence and absence of lipopolysaccharide (LPS) at 8 and 18 h. The analysis of the genetic material obtained from the cells was quantitated using real-time reverse transcription polymerase chain reaction (RT-PCR). The cell populations treated with LPS or PMMA microspheres singly resulted in an elevation of cytokine levels compared to the untreated control. LPS resulted in a 258-fold increase, while PMMA resulted in an 87.9-fold increase at 8 h. RAW 264.7 cells incubated with LPS and PMMA particles demonstrated a synergistic effect by producing a marked increase in the level of cytokine expression, 336-fold greater than that of the untreated control at 8 h. Fluorescence microscopy studies that assessed cellular viability were also performed and are consistent with the RT-PCR results. © 2004 Wiley Periodicals, Inc.* J Biomed Mater Res 69A: 305–313, 2004

Key words: cytokine; inflammatory; RT-PCR; biomaterials; wear debris

INTRODUCTION

The use of implanted medical devices is an essential component to the practice of medicine. Excluding dental implants and contact lenses, more than 3 million people in the United States have long-term biomedical implants, including breast prostheses, joint replacements, vascular grafts, pacemakers, and catheters.[1] Biomedical implants are comprised of a variety of biomaterials, most of which are inert and nontoxic. Despite these harmless characteristics, biomaterials trigger inflammatory responses after implantation. These responses are evidenced by an accumulation of phagocytic cells and by the production of cytokines.[1–3] The buildup of these phagocytic cells results in signal transduction that can culminate in diverse results, including device-mediated inflammation.[4] During the lifetime of the implant, wear debris particles are generated and phagocytosed by immune cells, causing inflammatory cascades to be propagated.[5–7] The cytokine family of proteins consists of a vast number of crucial regulator proteins. Cytokines are responsible for the initiation, mediation, and propagation of cellular inflammatory responses. In addition, they are involved in several other immune processes such as lymphocyte activation, proliferation, differentiation, angiogenesis, and apoptosis.[8,9] In addition, cellular inflammatory responses are enhanced by the presence of bacterial components or endotoxins. The critical segments of Gram-negative bacteria involved in inflammatory responses are lipopolysaccharide (LPS) molecules, which are liberated when the bacterial cell wall is degraded. Tumor necrosis factor (TNF) is one of the most prominent cytokines involved in mounting an immune response to Gram-negative bacteria. TNF exists in two isoforms: TNF-α and TNF-β. TNF-α is produced and secreted by several immune cells, whereas TNF-β is only produced bylymphocytes.[10] Another prominent cytokine involved in inflamma-

Correspondence to: L. Bailey; e-mail: leeann.bailey@nist.gov
Contract grant sponsor: NIST/NIDCR; contract grant number: Y1-DE-1021

tory responses due to the presence of LPS is interleukin-1 (IL-1). The parent polypeptide of IL-1 must be enzymatically processed to liberate the α- and β-subunits leading to subsequent biologic activation. IL-1β is the moiety of interest for these studies.

The transcriptional regulation of IL-1β and TNF-α is critical for cellular homeostasis and for the host to mount effective immune responses. The identification of the key cytokines involved is critical to understanding the cellular response and for the quantification of the cytokine(s) present. In most instances, the amount of sample tissue available to investigate cytokine levels is insufficient for protein analysis techniques such as enzyme-linked immunoassay (ELISA). Even if sufficient material is available, ELISA techniques are limited because of the variation in enzyme kinetics and because of the limit in the number of cytokines that can be analyzed simultaneously. As a result, the traditional methods used to evaluate small samples seek to quantitate mRNA levels.[8] There are four major methods commonly used to quantify mRNA expression: Northern blotting, *in situ* hybridization, RNase protection assays, and cDNA arrays. The main limitations of these assays are their low measure of sensitivity.[11,12]

Previous studies explored the relationship between macrophages, particle debris, and cytokine response using techniques such as ELISA.[13] These studies suggest that there is controversy and variation in cellular cytokine response depending upon the type of material and cell line used. It was hypothesized that endotoxin can bind tightly to the surfaces of materials and thus is one of the causal reasons for inflammatory responses.[14] Other studies indicate that serum proteins alone can bind to orthopedic debris and elicit macrophage activation and subsequent inflammatory responses.[15,16] These data validate the hypothesis that the type of protein adsorbed to the surface of the biomaterial is critical. In addition, the conformation of the protein on the surface also appears to modulate the interaction between the macrophage and the interface of the biomaterial surface.[13]

In our studies, we chose to quantify inflammatory cellular responses using real-time reverse transcription polymerase chain reaction (RT-PCR). Genetic regulation precedes protein production, and it is the goal of this work to improve upon quantification techniques in an accurate and well-characterized system. Real-time RT-PCR is an *in vitro* method for enzymatically amplifying defined sequences of RNA.[17] Further, it is the most sensitive, accurate, and adaptable of the mRNA quantitative techniques.[11] This technique can be used to amplify mRNA from one cell or from a large population of cells, such as tissue. Using a reverse transcriptase enzyme, RNA is converted to the cDNA template necessary for amplification. Once cDNA has been generated, gene-specific primers, a DNA polymerase, and a fluorescent moiety are utilized to amplify and subsequently label the amplicon generated. The product accumulation is then measured during the exponential phase of the reaction.[17] The copy number from the samples obtained can then be extrapolated back to a standard gene curve to yield quantitative data. The assay also includes the analysis of an mRNA that does not change in relative abundance during the course of treatment to serve as an internal control.[18]

RT-PCR can be used for a number of different applications. In this study we chose to characterize and compare the mRNA profiles of TNF-α and IL-1β in RAW 264.7 cells using RT-PCR. The 18 S ribosomal subunit was chosen as the housekeeping gene because its cellular concentration is fairly constant. These profiles were examined in samples that had been incubated in the presence or absence of LPS, 4.4-μm polymethylmethacrylate (PMMA) microspheres, or in combination. RAW 264.7 cells were chosen because they retain many of the functions of primary cultured macrophages, including the ability to phagocytose particles and release cytokines.[19–23] We hypothesized that greater levels of cytokine would be evident in cells that were incubated with polymer particles or stimulant in comparison to control sample levels. In addition, we wanted to characterize any synergy that might exist between the two treatments at the genetic level. Thus, the macrophage cultures were subjected to incubation with the above agents for different exposure times to probe cytokine levels.

MATERIALS AND METHODS

Cell lines

RAW 264.7 cells, a murine macrophage cell line, were purchased from American Type Culture Collection (ATCC, Manassas, VA) and maintained in RPMI (Life Technologies, Rockville, MD) supplemented with 10% (volume fraction) heat-inactivated fetal bovine serum (FBS) (Life Technologies) in 5% CO_2: 95% air at 37°C. To harvest, RAW 264.7 cells were washed with calcium- and magnesium-free phosphate-buffered saline and subsequently incubated with HANKS buffered salt solution without calcium or magnesium to promote release from the flask.

Treatment

RAW 264.7 (80,000–1,000,000) cells were plated and allowed to reach 70% confluency in a 75-cm^2 flask. To the culture, 0.01 mL of a PMMA microsphere suspension (1.915×10^9/mL) (Bangs Laboratories, Fishers, IN) was added and the cells were incubated for 24 h in a 10-mL

culture. The PMMA particles were in a sterile solution of deionized water containing 0.01% merthiolate solution. After 24 h, LPS (Sigma, St. Louis, MO) (1 μg/mL) *Escherichia coli* strain 026:B6 was added to the culture and the cells were incubated for either 8 or 18 h prior to the mRNA harvest. All of the particle suspensions and cell culture supernatant suspensions were tested for endotoxin using the Limulus Amebocyte Lysate Assay (Pyrogent Plus test kit, BioWhittaker, Walkersville, MD) with a sensitivity of 0.06 EU/mL.

mRNA extraction

Cells were plated in sterile 150 mm × 25-mm nonpyrogenic polystyrene dishes (Daigger, Vernon Hills, IL). Specific cultures were incubated with 4.4-μm PMMA microspheres or LPS either singly or in combination. The mRNA extraction was carried out using the materials and protocol provided in the Rneasy Kit from Qiagen (Qiagen, Valencia, CA). The protocol was followed according to the manufacturer's specification except a 21-gauge needle was used for homogenization of the sample. The RNA was immediately treated with RNA Secure after elution from the membrane (Ambion, Austin, TX) and stored at −20°C. Standard spectrophotometric measurements were taken and a 2% (mass fraction) agarose gel stained with 10 μg/mL ethidium bromide (Sigma) was used to image the RNA. Densitometry was performed using the Versa Doc imaging system (Bio-Rad, Hercules, CA).

Standards

The plasmids containing the cDNA inserts for TNF-α, interleukin-1β, and the 18 S ribosomal subunit were purchased from ATCC. The DNA had previously been cloned into a vector, which was introduced into an *E. coli* host. The *E. coli* expressing the DNA insert of choice was grown in LB medium. The plasmids were grown in LB medium (ATCC medium 1065) with 100 μg/mL of ampicillin for selection purposes. Plasmid DNA was isolated using the Qiagen Plasmid Giga Kit and no modifications were made to the manufacturer's protocol. Spectrophotometric measures were taken at 260 nm, and a 1% (mass fraction) agarose gel stained with 10 μg/mL ethidium bromide (Sigma) was used to image the DNA. Densitometry was performed using the Versa Doc imaging system.

Primer design

Primers were designed using Primerfinder (Whitehead Institute for Biomedical Research) for the RT-PCR experiments. The primers generated were used in both PCR and RT-PCR experiments. They are as follows: 18 S ribosomal subunit, 5′ agcgaccaaaggaaccataa 3′ and 3′ ctcctcctcctcctctctcg 5′; TNF alpha, 5′ tttcctcccaataccccttc 3′ and 3′ agtgcaaaggctccaaagaa 5′; IL-1 beta, 5′ tgtgaaatgccacctttga 3′ and 3′ gtagctgccacagcttctcc 5′. The amplicons generated from these primers are 204, 202, and 205 base pairs, respectively. DNA sequencing was performed using the Big Dye Terminator Kit (ABI, Foster City, CA) on a 310 DNA Genetic Analyzer (ABI).

RT-PCR

RT-PCR was carried out using the QuantiTect SYBR Green RT-PCR Kit and protocol (Qiagen) using an iCycler instrument (Biorad, Hercules, CA). The protocol utilizes the following thermal parameters: reverse transcription, 30 min at 50°C; activation step, 15 min at 95°C; three-step cycling, denaturation for 30 s at 95°C, annealing for 2 min at 57°C, extension for 2 min at 72°C for 35 cycles. A melt curve was subsequently performed to analyze the products generated, which began at 50°C and increased to 95°C in 1°C increments.

Fluorescence microscopy

RAW 264.7 cells were plated at a density of 20,000 cells/well in 0.25 mL of RPMI medium in a 24-well plate. The next day, cells were treated with PMMA microspheres and allowed to phagocytose the particles for 24 h. Finally, the cells were treated with LPS for the appropriate length of time. Prior to analysis, the medium was removed from the culture and the cells were washed with 1 mL of medium. The cells were "Live–Dead" stained by adding 0.5 mL of medium containing 0.002 m*M*/L calcein-AM and 0.002 m*M*/L ethidium homodimer-1 (both from Molecular Probes, Eugene, OR). The cells were incubated for 5 min, observed by epifluorescence microscopy, and photographed. The ratio of PMMA microspheres to cells was kept constant and represented a smaller model of the larger treated samples generated for mRNA harvest.

RESULTS AND DISCUSSION

The RT-PCR method of quantification used in these studies is the standard curve method. In the standard curve method samples of known concentrations are used to construct a calibration plot.[8] The constructs used for standard curve generation were cDNA plasmids. The concentration of each construct was determined using both densitometry and spectrophotometric techniques (data not shown). The standard curve efficiencies for all of the constructs used in these studies were 80 ± 5. The RT-PCR reactions were run in parallel with standard constructs and appropriate controls.

SYBER Green I is a fluorescent dye that becomes incorporated into the amplicon during the reaction. This dye binds to all double-stranded DNA molecules

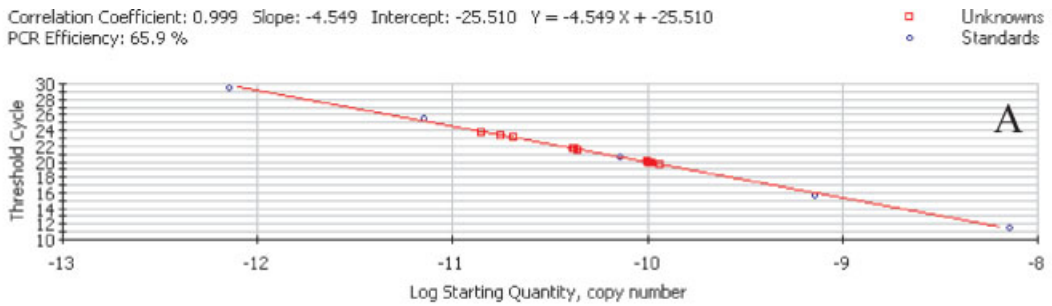

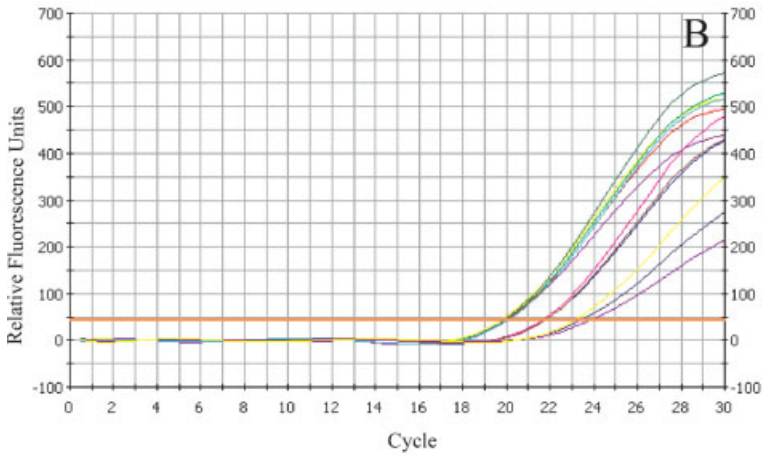

SAMPLE	Mean Ct	Log of Starting Quantity	Starting Quantity Standard Deviation
TNF-α Standard 1	11.42	8.149	N/A
TNF-α Standard 2	15.34	9.149	N/A
TNF-α Standard 3	20.20	10.149	N/A
TNF-α Standard 4	25.24	11.149	N/A
TNF-α Standard 5	28.91	12.149	N/A
LPS & PMMA	19.43	9.972	1.01×10^{-11}
LPS	19.53	9.995	3.07×10^{-12}
PMMA	21.20	10.367	1.19×10^{-12}
Untreated Control	22.87	10.782	2.72×10^{-12}

Figure 1. Standard curve with samples along with the amplification plots of samples. The standard curve in (A) displays a plot of cDNA standards and cellular samples are shown with the best-fit curve. In (B) the triplicate runs of the cellular samples are shown and the results are summarized in the table. [Color figure can be viewed in the online issue, which is available at www.interscience.wiley.com.]

and emits a fluorescent signal upon binding. This fluorescence is measured and displayed in the amplification plots. The standard curves are comprised of serial tenfold dilutions; these dilution series encompass the concentration range of the samples. Figure 1 examines the cytokine data generated for TNF-α at 8 h. Figure 1(A) displays the cDNA standards and the location of the samples on the standard curve. Figure 1(B) demonstrates the amplification plot of the RAW 264.7 samples only. The untreated control samples and the samples incubated with PMMA alone have overlapping critical threshold (C_t) values. Further, the samples incubated with LPS singly or with LPS and PMMA in concert have similar C_t values. Each experimental sample was run in triplicate, and each is comprised of three different cell populations. Thus, these samples demonstrate that it is possible to get reproducible data from different populations of cells. The table adjacent to Figure 1(B) displays the numerical values generated from the amplification plot. These values were later used to construct Figures 3 and 4. The RT-PCR efficiency value appears to be lower than stated earlier; however, this value can change depending upon baseline and threshold parameters. To make an exact comparison between samples, the threshold was held constant at 44.6 relative fluorescence units.

A common experimental problem in RT-PCR is the presence of excess primer in the reaction. Often, the primers will begin to interact with one another and generate "primer–dimers." These moieties can emit fluorescence that is not indicative of the amplicon of interest. A melt curve was performed (Fig. 2) to ensure that the fluorescence being measured was specific to the gene being amplified and that excess primer was not present. The melting temperature of the primers is between 65–72°C; thus, if a structure (primer–dimer) formed and SYBER Green I was incorporated into them a peak would be present in that region of the melting curve. Figure 2 demonstrates that the product generated was specific in all samples. DNA sequencing validated that the product generated was the sequence of interest (data not shown). Gel electrophoresis further validated the specificity of the product and provided an endpoint measurement of the sample (data not shown). RAW 264.7 cytokine profiles were investigated to determine the cellular inflammatory

responses exhibited. The results for the 8-h time point are shown in Figure 3. Pairwise comparisons were performed and, in Figure 3, the *p* values are shown above the diagonal in the table and the increases in cytokine expression between samples are shown below the diagonal. The cells incubated with PMMA microspheres exhibited an increase in cytokine expression, as did the cells incubated with LPS. The cellular response to LPS was greater than control levels. The greatest increase was exhibited by the sample that was incubated in the presence of both LPS and PMMA microspheres. The levels of TNF-α were roughly the same in the population treated with LPS singly (5.5-fold increase) and the population treated with both LPS and PMMA (5.8-fold increase) in comparison to control levels. Further, IL-1β levels were elevated significantly in comparison to TNF-α levels. The samples

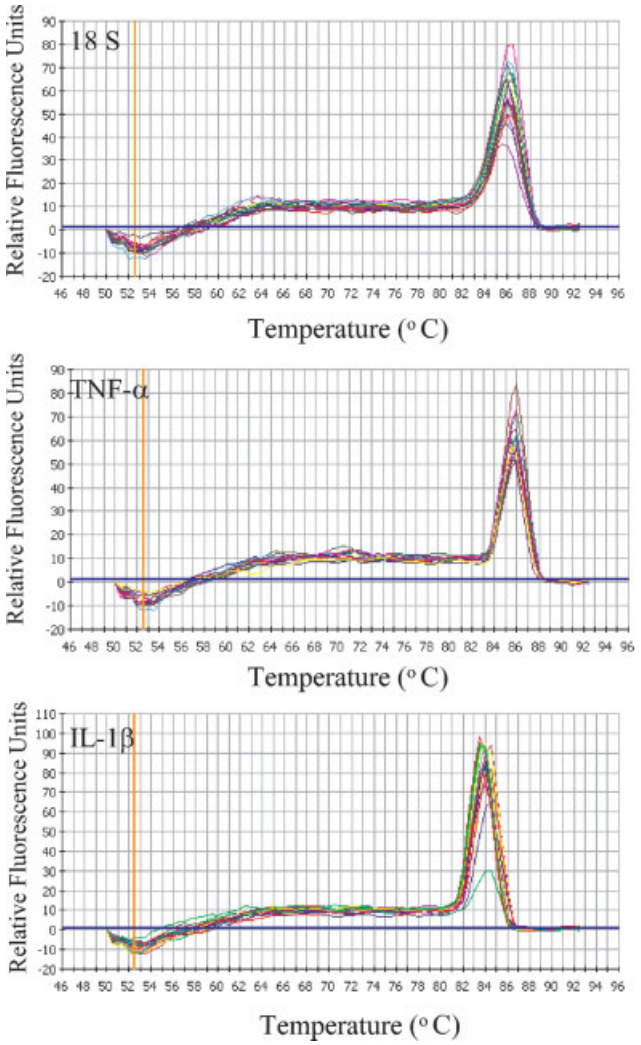

Figure 2. Melt curves for each gene product generated during RT-PCR experiments. The standard uncertainty is estimated to be 2%, which is based on the standard deviation of multiple measurements. [Color figure can be viewed in the online issue, which is available at www.interscience.wiley.com.]

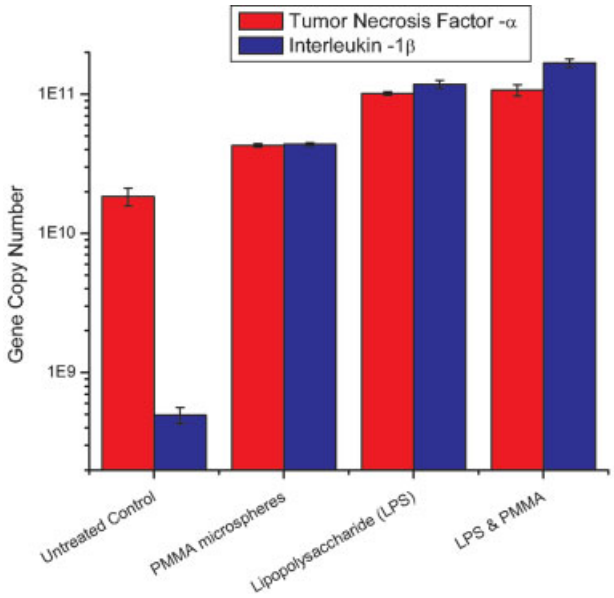

SAMPLE	Control	PMMA	LPS	PMMA & LPS
TNF-α /Control	---------	p < 0.0004	p < 0.000002	p < 0.003
TNF-α/ PMMA	2.33	----------	p < 0.00005	p < 0.005
TNF-α/ LPS	5.50	2.36	----------	p < 0.3
TNF-α/ PMMA & LPS	5.82	2.49	1.06	----------

SAMPLE	Control	PMMA	LPS	PMMA & LPS
IL-1β /Control	---------	p < 0.0002	p < 0.0006	p < 0.0008
IL-1β / PMMA	87.9	---------	p < 0.002	p < 0.002
IL-1β /LPS	258	2.93	----------	p < 0.004
IL-1β /PMMA & LPS	336	3.82	1.30	----------

Figure 3. Gene copy number of IL-1β and TNF-α after 8 h of treatment. Pairwise comparisons were performed and the *p* values are shown on the top diagonal in the tables; the bottom diagonal reports the relative increase in cytokine expression between samples. Error bars are representative of one standard deviation from the mean of triplicate samples harvested from three separate populations of RAW 264.7 cells and is the estimate of the standard uncertainty. [Color figure can be viewed in the online issue, which is available at www.interscience.wiley.com.]

that were treated with LPS and PMMA exhibited high levels of IL-1β, 336-fold more in comparison to untreated control levels. The samples incubated with LPS yielded a 258-fold increase, and PMMA alone yielded an 87.9-fold increase in comparison to untreated control levels. Thus, the RAW 264.7 population treated with LPS and PMMA to simulate the conditions *in vivo* resulted in a synergistic elevation of IL-1β cytokine levels and a marked increase in TNF-α compared to basal levels.

The cellular cytokine profile was also investigated at 18 h (Fig. 4). Again, pairwise comparisons were performed and the *p* values are shown above the diagonal in the table and the increases in cytokine expression between samples are shown below the diagonal (Fig. 4). At the 18-h time point, the levels of TNF-α appeared to have returned to the basal level expression.

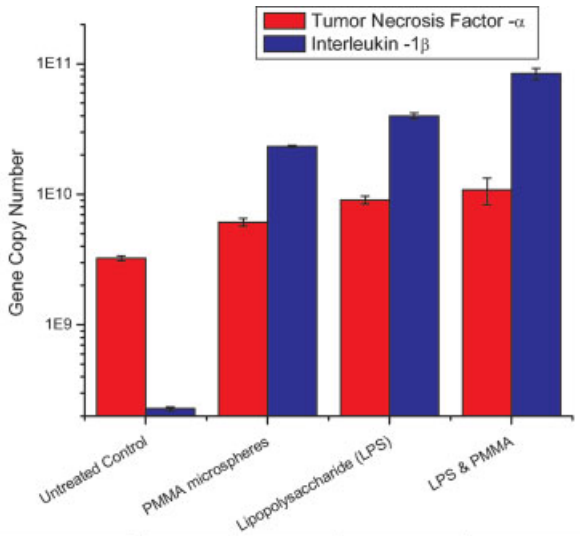

SAMPLE	Control	PMMA	LPS	PMMA & LPS
TNF-α /Control	--------	p < 0.004	p < 0.003	p < 0.02
TNF-α/ PMMA	1.89	--------	p < 0.002	p < 0.02
TNF-α/ LPS	2.79	1.48	--------	p < 0.05
TNF-α/ PMMA & LPS	3.33	1.77	1.2	--------

SAMPLE	Control	PMMA	LPS	PMMA & LPS
IL-1β /Control	---------	p < 0.0005	p < 0.0006	p < 0.002
IL-1β / PMMA	102	----------	p < 0.004	p < 0.004
IL-1β /LPS	173	1.70	----------	p < 0.002
IL-1β /PMMA & LPS	368	3.61	2.12	----------

Figure 4. Gene copy number of IL-1β and TNF-α after 18 h of treatment. Pairwise comparisons were performed and the *p* values are shown on the top diagonal in the tables; the bottom diagonal reports the relative increase in cytokine expression between samples. Error bars are representative of one standard deviation from the mean of triplicate samples harvested from three separate populations of RAW 264.7 cells and is the estimate of the standard uncertainty. [Color figure can be viewed in the online issue, which is available at www.interscience.wiley.com.]

The quantity of this cytokine changed little in comparison to untreated control levels (Fig. 4). In contrast, IL-1β levels continued to be elevated similar to the 8-h time point, although the level measured at 18 h had decreased to roughly half that of the earlier time point. These results are consistent with the work of Baer et al.,[24] who observed a sharp increase in TNF-α expression by macrophages after exposure to LPS followed by a steady decrease over 8 h. In contrast, IL-1β levels were relatively constant, or actually increased steadily, depending on the culture medium. These authors attributed this temporal profile of TNF-α to a regulatory element they termed TNF-α-inhibiting factor (TIF), which selectively suppresses expression of this cytokine. Baer et al. suggested that TIF acts through an autocrine mechanism in concert with NF-κB p50 and it is this factor that is directly responsible for repressing the TNF-α promoter.

There are several possibilities to explain these data (Figs. 3 and 4). The first is that RAW 264.7 cells were regulating cytokine production in response to signal transduction occurring within the population.[25] It is well documented that a variety of cytokines play roles in mounting inflammatory responses.[1,26] Further, it has been documented that there is a temporal sequence in which immune cells respond to inflammatory signals.[27] Perhaps the macrophages were regulating which cytokine was expressed and what quantity was produced for a discrete period of time. Another hypothesis is that the cells were no longer viable due to excessive phagocytosis and an increase in the production of proinflammatory cytokines. The decline in viability within the population could be responsible for the decreased levels of cytokine. To investigate the second hypothesis, fluorescence microscopy was used to assess cellular viability.

To assess the cellular viability of the RAW 264.7 cell populations, we utilized a fluorescence assay (Fig. 5). The principle of the assay is that membrane-permeant calcein AM is cleaved by esterases in live cells to yield cytoplasmic green fluorescence and membrane-impermeant ethidium homodimer-1 labels nucleic acids of membrane-compromised cells with red fluorescence. Thus, live cells fluoresce green and dead cells fluoresce red. Figure 5 illustrates RAW 264.7 populations at a 40×magnification to display the morphological characteristics of the cells. Figure 5(A) displays a phase-contrast image of RAW 264.7 cells, and figure 5(B) illustrates the same sample labeled with the fluorescent probes at 18 h. The entire panel [Fig. 5(B)] was green, indicating that the population was viable. Figure 5(C) depicts a phase-contrast image of RAW 264.7 cells that have phagocytosed 4.4-μm PMMA microspheres and Figure 5(D) displays the same sample labeled with the fluorescent probes. Figures 5(C) and 5(D) depict cells with a rounded morphology and maximal phagocytosis. Despite this extreme condition panel D was green, indicating that the majority of the population was viable at 18 h. The same procedure was repeated for cells incubated with LPS and for cells incubated with both LPS and PMMA at the 8-h time point. At the 8-h time point the control populations and the populations incubated with either PMMA microspheres or LPS were viable with levels of red fluorescence comparable to Figure 5(E) (data not shown). The population treated with both LPS and PMMA microspheres at 8 h appeared to be compromised minimally (data not shown).

To demonstrate population viability, the above experiment was repeated and images were captured at a 10× magnification. The data are shown in Figure 6. Figures 6(A), 6(C), 6(E), and 6(G) represent the viable cells within the population and Figures 6(B), 6(D), 6(F), and 6(H) represent the cells that were not viable within the population. These data illustrate that populations treated singly with either LPS or PMMA mi-

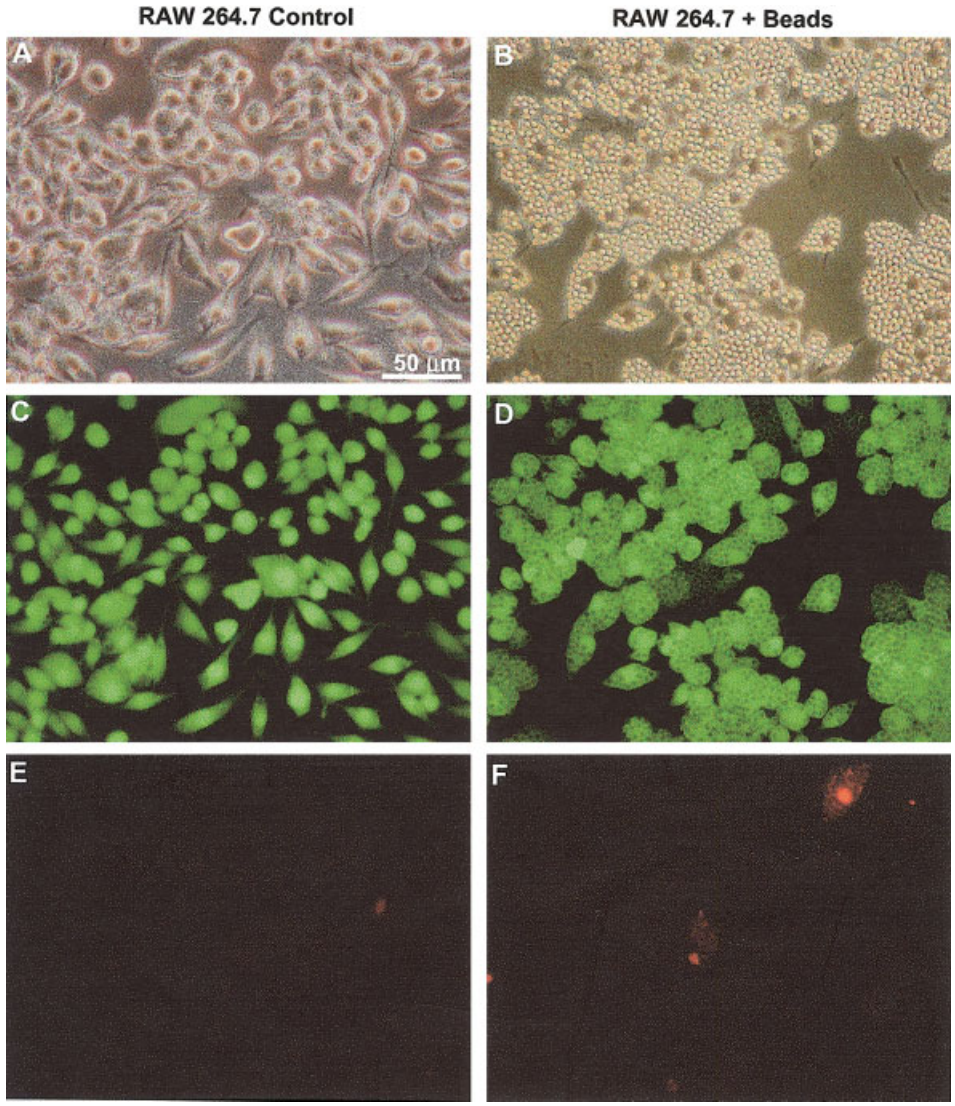

Figure 5. Fluorescence microscopy of RAW 264.7 cells stained with live/dead fluors after 8 h. (A) Phase-contrast image of untreated cells. (B) Untreated cells stained with fluors. (C) Phase contrast image of RAW 264.7 cells incubated with PMMA microspheres for 8 h. (D) RAW 264.7 cells incubated with PMMA microspheres for 8 h, and stained with fluors. [Color figure can be viewed in the online issue, which is available at www.interscience.wiley.com.]

crospheres exhibited a small decline in viability. However, the population treated with both agents demonstrated that a large number of cells in the population were no longer viable at 18 h. These data further reinforce the RT-PCR data. Further, it is feasible that the increased number of nonviable cells resulted in a less robust cytokine expression profile in the 18-h RAW 264.7 population. Thus, we conclude that a decline in viability coupled with transcriptional regulation can lead to a decreased level of cytokine production.

CONCLUSION

The molecular mechanisms and signal transduction that occur during inflammatory responses are complex. In addition, the mechanisms regarding the initiation and propagation of inflammatory responses are not well defined at present. Several cytokines are known to play prominent roles in the propagation and mediation of inflammatory responses, and we developed a model system that mimics device-mediated inflammation *in vivo.* RT-PCR is a quantitative technique that accurately measures the gene copy number present in samples of many different types. Caveats to utilizing SYBER Green I, as opposed to specific primers and probes, is that multiplexing is not possible and it is difficult to quantitate small differences in gene expression. Another difficulty concerns the establishment of the baseline and threshold parameters and the effect that changing these values has on the results. While the trends of the data ultimately are unchanged,

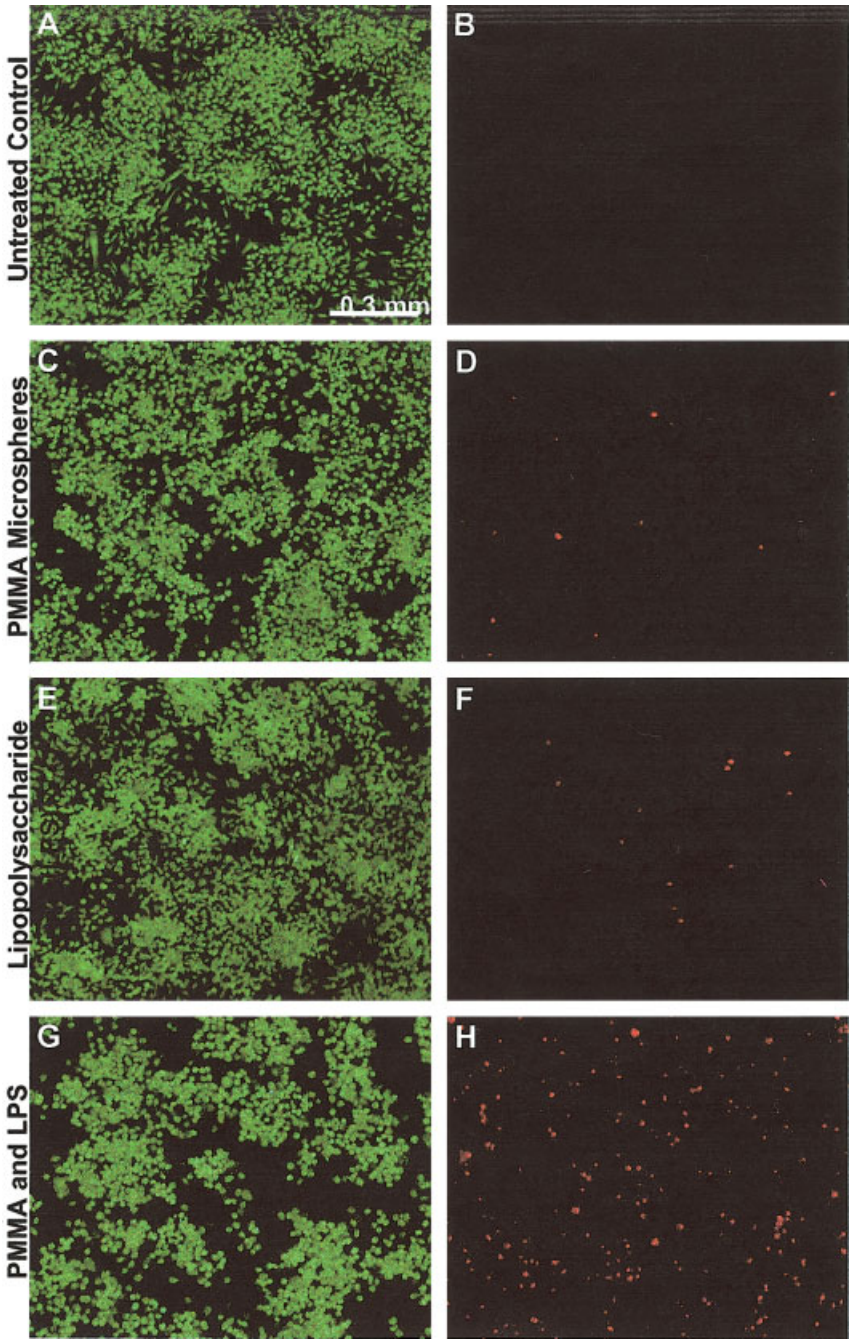

Figure 6. Fluorescence microscopy of RAW 264.7 cells stained with live/dead fluors after 18 h. (A, B) Untreated controls. (C, D) Cells incubated with PMMA microspheres. (E, F) Cells incubated with LPS. (G, H) Cells incubated with both LPS and PMMA microspheres. [Color figure can be viewed in the online issue, which is available at www.interscience.wiley.com.]

the numbers can shift ±5% by varying these experimental parameters.

We successfully applied RT-PCR to measure the inflammatory responses of RAW 264.7 macrophages and follow the induction of IL-1β and TNF-α production. Our results suggest that micrometer-scale PMMA beads and LPS are capable of inducing cytokine transcription but have a synergistic effect only when exposed to macrophages together. The time dependence of gene upregulation was different for IL-1β and TNF-α, with TNF-α levels dropping off after 18 h but IL-1β levels remaining significantly higher than those measured from untreated cells. Our data validate earlier studies[15,16] regarding protein adsorption to biomaterials and the ability of this complex to modulate cellular inflammatory responses. PMMA particles were capable of stimulating cytokine production without the presence of LPS and the data were statistically significant. In summary, we conclude that the RAW 264.7

macrophages comprise an *in vitro* model that allows for insights regarding cellular inflammatory responses.

This work was partially funded by the NIST/NIDCR Interagency Agreement (Y1-DE-1021).

References

1. Tang L, Eaton JW. Inflammatory responses to biomaterials. Am J Clin Pathol 1995;103:466–471.
2. Tang L, Ugarova TP, Plow EF, Eaton JW. Molecular determinants of acute inflammatory responses to biomaterials. J Clin Invest 1996;97:1329–1334.
3. Tang L, Lucas AH, Eaton JW. Inflammatory responses to implanted polymeric biomaterials: role of surface-adsorbed immunoglobulin G. J Lab Clin Med 1993;122:292–300.
4. Abbas AK, Lichtman AH, Pober JS. Cellular and molecular immunology, 2nd ed. Philadelphia: W. B. Saunders, 1994.
5. Rodrigo AM, Martinez ME, Saldana L, Valles G, Martinez P, Gonzalez-Carrasco JL, Cordero J, Munuera L. Effects of polyethylene and alpha-alumina particles on IL-6 expression and secretion in primary cultures of human osteoblastic cells. Biomaterials 2002;23:901–908.
6. Goering PL, Kuester RK, Neale AR, Chapekar MS, Zaremba TG, Gordon EA, Hitchins VM. Effects of particulate and soluble cadmium species on biochemical and functional parameters in cultured murine macrophages. In Vitro Mol Toxicol 2000;13:125–136.
7. Ingham E, Green TR, Stone MH, Kowalski R, Watkins N, Fisher J. Production of TNF-alpha and bone resorbing activity by macrophages in response to different types of bone cement particles. Biomaterials 2000;21:1005–1013.
8. Giulietti A, Overbergh L, Valckx D, Decallonne B, Bouillon R, Mathieu C. An overview of real-time quantitative PCR: applications to quantify cytokine gene expression. Methods 2001;25:386–401.
9. Oppenheim JJ. Cytokines: past, present, and future. Int J Hematol 2001;74:3–8.
10. Pauli U. Control of tumor necrosis factor gene expression. Crit Rev Eukaryot Gene Expr 1994;4:323–344.
11. Wang T, Brown MJ. mRNA quantification by real time TaqMan polymerase chain reaction: validation and comparison with RNase protection. Anal Biochem 1999;269:198–201.
12. Melton DA, Krieg PA, Rebagliati MR, Maniatis T, Zinn K, Green MR. Efficient in vitro synthesis of biologically active RNA and RNA hybridization probes from plasmids containing a bacteriophage SP6 promoter. Nucleic Acids Res 1984;12:7035–7056.
13. Daniels AU, Barnes FH, Charlebois SJ, Smith RA. Macrophage cytokine response to particles and lipopolysaccharide in vitro. J Biomed Mater Res 2000;49:469–478.
14. Bi Y, Seabold JM, Kaar SG, Ragab AA, Goldberg VM, Anderson JM, Greenfield EM. Adherent endotoxin on orthopedic wear particles stimulates cytokine production and osteoclast differentiation. J Bone Miner Res 2001;16:2082–2091.
15. Maloney JW, Nakashima Y, Sun DH, Smith RL. Human serum and TiAIV particles: Protein binding and macrophage activation. Trans Orthop Res Soc 1996;21:68.
16. Sun DH, Nakashima Y, Maloney WJ, Goodman SB. Opsonization of particulate debris: Protein identification by 2-d gel analysis. Trans Orthop Res Soc 1997;22:324.
17. Bustin SA. Absolute quantification of mRNA using real-time reverse transcription polymerase chain reaction assays. J Mol Endocrinol 2000;25:169–193.
18. Suzuki T, Higgins PJ, Crawford DR. Control selection for RNA quantitation. Biotechniques 2000;29:332–337.
19. Chapekar MS, Zaremba TG, Kuester RK, Hitchins VM. Synergistic induction of tumor necrosis factor alpha by bacterial lipopolysaccharide and lipoteichoic acid in combination with polytetrafluoroethylene particles in a murine macrophage cell line RAW 264.7. J Biomed Mater Res 1996;31:251–256.
20. Funatogawa K, Matsuura M, Nakano M, Kiso M, Hasegawa A. Relationship of structure and biological activity of monosaccharide lipid A analogues to induction of nitric oxide production by murine macrophage RAW264.7 cells. Infect Immunol 1998;66:5792–5798.
21. Jue DM, Sherry B, Luedke C, Manogue KR, Cerami A. Processing of newly synthesized cachectin/tumor necrosis factor in endotoxin-stimulated macrophages. Biochemistry 1990;29:8371–8377.
22. Raschke WC, Baird S, Ralph P, Nakoinz I. Functional macrophage cell lines transformed by Abelson leukemia virus. Cell 1978;15:261–267.
23. Tiffany CW, Burch RM. Bradykinin stimulates tumor necrosis factor and interleukin-1 release from macrophages. FEBS Lett 1989;247:189–192.
24. Baer M, Dillner A, Schwartz RC, Sedon C, Nedospasov S, Johnson PF. Tumor necrosis factor alpha transcription in macrophages is attenuated by an autocrine factor that preferentially induces NF-kappaB p50. Mol Cell Biol 1998;18:5678–5689.
25. Raabe T, Bukrinsky M, Currie RA. Relative contribution of transcription and translation to the induction of tumor necrosis factor-alpha by lipopolysaccharide. J Biol Chem 1998;273:974–980.
26. Catelas I, Huk OL, Petit A, Zukor DJ, Marchand R, Yahia L. Flow cytometric analysis of macrophage response to ceramic and polyethylene particles: effects of size, concentration, and composition. J Biomed Mater Res 1998;41:600–607.
27. Anderson JM. Biological responses to materials. Annu Rev Mater Res 2001;31:81–110.